ISSN 0018-1439, High Energy Chemistry, 2017, Vol. 51, No. 5, pp. 381–389. © Pleiades Publishing, Ltd., 2017.
Original Russian Text © V.A. Livshits, B.B. Meshkov, V.G. Avakyan, B.G. Dzikovskii, M.V. Alfimov, 2017, published in Khimiya Vysokikh Energii, 2017, Vol. 51, No. 5, pp. 398–406.

NANOSTRUCTURED SYSTEMS AND MATERIALS

# Structure and Molecular Dynamics of Host–Guest Complexes of TEMPO with Cucurbituryl: An ESR and DFT Study

**V. A. Livshits[a, b, *], B. B. Meshkov[a], V. G. Avakyan[a], B. G. Dzikovskii[a], and M. V. Alfimov[a, b]**

[a] *Photochemistry Center "Crystallography and Photonics", Russian Academy of Sciences, Moscow, 119421 Russia*

[b] *Moscow Institute of Physics and Technology, Dolgoprudnyi, Moscow oblast, 141701 Russia*

**e-mail: vlivshi@mail.ru*

Received December 5, 2016

**Abstract**—Host–guest complexes are of interest as promising nanodevices for molecular recognition and chemosensors. In this work, the structure and molecular dynamics of complexes of the nitroxyl radical TEMPO (**I**), as models of indicator and analyte, with cucurbituril CB[7] in solution and in the solid phase have been studied by ESR and DFT methods. The kinetic accessibility of the NO group of **I** for water-soluble reagents has been determined. By simulation of the ESR spectra of the complex, the rotational diffusion coefficients and the anisotropy of its rotation have been determined. To study the rotational mobility of the guest in the CB[7] cavity, solid solutions of **I**@CB[7] in the CB[7] matrix have been obtained. The ESR spectra indicate rapid jump-like rotation of **I** about an axis oriented along the normal to the CB[7] portals. The formation energy and the spatial structure of the complex have been calculated by the DFT method; a change in the spin density on the NO group with changing the orientation of **I** in the CB[7] cavity has been found.

*Keywords:* host–gest complexes, cucurbiturils, rotational dynamics, nitroxyl radicals, DFT calculations

**DOI:** 10.1134/S0018143917050083

Cucurbiturils (cucurbit[-n]urils, CB[n]), a new class of supramolecular host molecules, have attracted much attention in recent years due to their ability to form stable and selective host–gest (HG) complexes with various organic molecules and cations in aqueous medium [1, 2]. It was also shown that the photophysical properties of guest molecules, primarily fluorescence, often change significantly upon inclusion in CB[n] cavities [3–5]. These properties make it possible to use CB[n] as artificial receptors in chemo- and biosensors, drug carriers, photoswitches, and nanomotors [6–8].

Various methods were used to study HG complexes. The use of spin-labeled guests as models of analytes is of particular interest, since the analysis of the ESR spectra of the complexes permits determining the structure, thermodynamics, the kinetics of their formation, and the polarity of guest environment in the CB cavities [9–13].

Fundamentally important for the functioning of HG complexes are their dynamic properties: molecular mobility of guests in the CB[n] cavities, and their accessibility for water and water-soluble reagents. However, these properties, as far as we know, have not been sufficiently studied [13]. In the present work, the structure and molecular dynamics of CB [7] complexes with the nitroxyl radical TEMPO (**I**, see Scheme) were studied in aqueous solution and in the solid phase. The polarity of the environment of **I** in the complexes was determined from the hyperfine coupling (HFC) with the $N^{14}$ nucleus of the NO group. The accessibility of the NO group for paramagnets in water was determined from the broadening of the ESR spectra due to spin exchange.

To study the rotational dynamics of the spin probe inside the cavity, it is necessary to eliminate rotation of the complexes as a whole. For this purpose, magnetically dilute solutions of the complexes **I**@CB [7] were prepared in a solid matrix of CB [7] molecules. Rapid anisotropic rotation of **I** in the CB [7] cavity about the $Y$ axis in the system of the principal axes of the $A, g$ tensors was detected, with the $Y$ axis oriented parallel to the $C_7$ symmetry axis of CB [7].

Computer calculations of the structure of the complexes by the DFT method with a version of the method allowing for the van der Waals interaction were also carried out. The formation energies of the complexes at different orientations of **I** and the barrier of rotation of **I** about the $Y$ axis were determined; changes in the spin density on the atoms of the NO group with changing the orientation of **I** in the CB [7] cavity were found.

## EXPERIMENTAL

Cucurbituril CB [7] (Sigma–Aldrich) was used without further purification. 2,2,6,6-Tetramethylpiperidine-1-oxyl (TEMPO (**I**), see Scheme) was synthesized according to the previously published procedure [14].

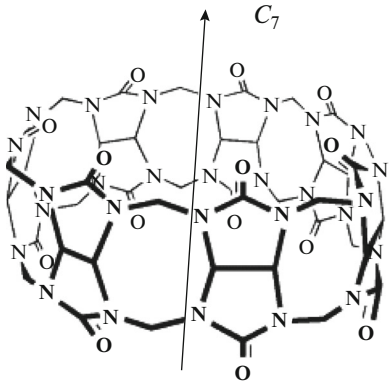


CB7

Cucurbit[7]uril (CB [7])

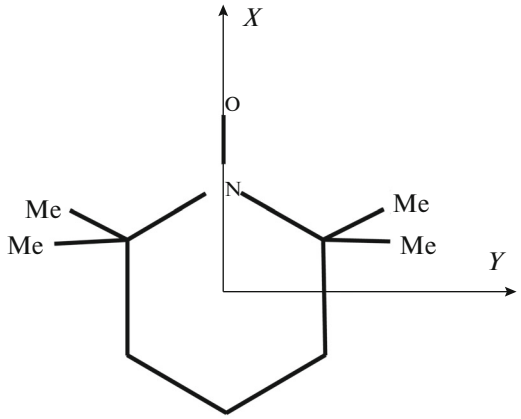


The Z axis is directed perpendicular to the *XY* plane

**Scheme 1.**

The *X*-band ESR spectra (frequency 9.15 GHz) were measured on an EPR-200 spectrometer (Bruker) under temperature control with a flow of evaporated nitrogen. The samples in the form of capillaries were located along the symmetry axis of a quartz tube containing silicone oil to provide thermal contact. The vertical size of the sample was no more than 5–6 mm, in order to avoid the inhomogeneity of the microwave field and the modulation field. All the spectra were recorded under the conditions of critical coupling of the resonator with the microwave line [15].

The ESR spectra were simulated using a program based on the stochastic Liouville equation and the method of nonlinear least squares [16, 17]. The $A_{zz}$ and $g_{zz}$ components of the HFC tensors and the *g* factor in the absence of rotation, necessary for simulation of the ESR spectra, were determined from the ESR spectra at 77 K.

Calculations of the structure of the complexes and the formation energies were carried out with complete optimization of the geometry, using the DFT-D3 method with the PBE functional in the SVP basis in the context of ORCA (version 3.0.1) software package [18], with allowance for the Grimme dispersion correction [19–21]. The HyperChem 8.0 package was used to obtain the initial structures and visualization of the results. The total energy of complex formation ($\Delta E_{total}$, where $E = E_{electron} + E_{vdW}$) was determined from Eq. (1):

$$\Delta E_{total} = E_{comp} - E_{\mathbf{I}} - E_{CB[7]}, \quad (1)$$

where $E_{comp}$, $E_{\mathbf{I}}$, and $E_{CB[7]}$ are the calculated energies of the complex, radical **I**, and CB[7], respectively. The van der Waals energy of complex formation was calculated from Eq. (2):

$$\Delta E_{vdW} = E_{vdW,\,comp} - E_{vdW,\,\mathbf{I}} - E_{vdW,\,CB[7]}, \quad (2)$$

where $E_{vdW,\,comp}$, $E_{vdW,\,\mathbf{I}}$, and $E_{vdW,\,CB[7]}$ are the calculated van der Waals energies of the complex of radical **I** with CB [7]. Tables 3 and 4 present the results of the calculations.

## RESULTS AND DISCUSSION

### *Properties of the Host–Guest Complexes I@CB [7] in Aqueous Solutions*

The binding constant of the complex **I**@CB [7], determined by subtracting the spectrum of free **I,** and the value of isotropic HFC $a_N$ characterizing the polarity of the environment of **I** are in agreement with the data of the work [9].

**Rotational diffusion of the complexes in aqueous solution.** The ESR spectra of the complex **I**@CB [7] were recorded at a CB [7] concentration of 6 mmol $L^{-1}$ and a molar ratio CB [7]/**I** = 60, which corresponds to complete binding of **I** at 292 K. The spectra were simulated in terms of the model of anisotropic Brownian rotational diffusion, using the method of nonlinear least squares [16, 17]. The best fitting was obtained for the model of an axially symmetric diffusion tensor with the symmetry axis of rapid rotation coinciding with the *Y* axis in the system of the principal axes of the *A* and *g* tensors (see Scheme). The characteristic fea-

**Table 1.** Polarity parameters of the environment of the NO group of **I** in the complex **I**@CB [7] in aqueous solution (292 K) and in the solid CB [7] matrix (77 K). The isotropic HFC constants $a_N$ (G) in the complex **I**@CB [7] ($a_N^{cb}$) in aqueous solution, **I** in water ($a_N^W$) and toluene ($a_N^T$) were determined as the distances between the HFC components $m = +1$ and $m = 0$; the polarity parameter in aqueous solution of **I**@CB [7] $p_{solut} = (a_N^{cb} - a_N^T)/(a_N^W - a_N^T)$. The components $A_{zz}$ (G) at 77 K for **I**@CB [7] in the CB [7] matrix and in frozen solutions of **I** in water and toluene were determined as half the distance between the terminal extremums of the ESR spectra. The polarity parameter in the solid phase $p_{solid} = (A_{zz}^{cb} - A_{zz}^T)/(A_{zz}^W - A_{zz}^T)$

| $T$ (K), environment | Spectral parameters (G) | Complex **I**@CB [7] | Water | Toluene | Polarity parameter |
|---|---|---|---|---|---|
| 290, water | $a_N$ | 16.01 | 17.21 | 15.36 | $p_{solut}$ 0.35 |
| 77, CB [7] matrix | $A_{zz}$ | 35.05 | 37.21 | 35.3 | $p_{solid}$ −0.13 |

**Table 2.** Exchange broadenings of the components of the hyperfine structure in the ESR spectra of **I**@CB [7] and free **I** at different concentrations of $C_{rox.}$ $T = 292$ K

| Crox (mmol $L^{-1}$) | Complex | $\Delta\omega_{free}^{ex}\left(s^{-1}\right)$ | $\Delta\omega_{comp}^{ex}\left(s^{-1}\right)$ | $\Delta\omega_{com}^{ex}/\Delta\omega_{free}^{ex}$ |
|---|---|---|---|---|
| 5 | **I**@CB [7] | $0.73 \times 10^7$ $s^{-1}$ | $0.1 \times 10^7$ $s^{-1}$ | 0.14 |
| 10 | | $1.97 \times 10^7$ $s^{-1}$ | $0.24 \times 10^7$ $s^{-1}$ | 0.13 |

tures of the spectra for this type of rotation are practically equal intensities of the components $m = \pm 1$ and the more intense component $m = 0$ (see Fig. 1 and [22]). The values of the parameters $R_\perp$ and $R_\parallel$ are $6.3 \times 10^8$ and $3.5 \times 10^{10}$ $s^{-1}$, respectively. The much larger $R_\parallel$ value in comparison with $R_\perp$ and, hence, the much larger ratio $R_\parallel/R_\perp$ than the ratio of the geometric dimensions of CB [7] may be explained by the existence of rotational mobility of the guest inside the CB [7] cavity (this mobility is studied in more detail in the next section by using immobilization of the complexes **I**@CB [7] in the CB [7] matrix).

**Polarity of the local environment of the NO group in aqueous solution of I@CB [7].** The polarity of the environment of the NO group is an important parameter that can give information about the location of the spin probe in the complex and the efficiency of chemical and photochemical processes in the CB [7] cavity. To characterize the polarity of the environment of the NO group in the complex, the value of the isotropic HFC constant in the complex ($a_N^{cb}$) and the values of $a_N$ in polar (water) and nonpolar (toluene) solvents, $a_N^W$ and $a_N^T$, respectively, were measured. From these values, it is possible to make a dimensionless polarity parameter $p_{solut} = (a_N^{CB} - a_N^T)/(a_N^W - a_N^T)$, which permits comparing the polarities of the environment for different media, complexes, and different probes. It is equal to 1 in water and 0 in toluene. The values of $a_N$ and $p_{solut}$ in **I**@CB [7] are given in Table 1. It can be seen from these values that the environment of the NO group in the complex **I**@CB [7] is relatively hydrophobic, that is, it is removed from contact with water.

**Kinetic accessibility of the NO group for water-soluble paramagnetic complexes**. The degree of accessibility of the NO group to water-soluble reagents is also an important parameter, which, along with the polarity of the environment, permits estimating the location of this group in the supramolecular complex. The kinetic accessibility of the NO group for water-soluble reagents can be determined by measuring the spin exchange with paramagnetic ions [23]. For this purpose, we studied the spin exchange of the complex **I**@CB [7] with water-soluble salts, potassium trioxalate chromate $K_3[Cr(ox)_3]^{3-}$ (Crox), which is known to produce the maximum exchange broadening in the ESR spectra of nitroxyl radicals [24], and potassium

**Table 3.** Total ($\Delta E_{total}$) and van der Waals ($\Delta E_{vdW}$) energies of formation of the complex **I**@CB [7] for two orientations of **I** in the CB [7] cavity (kcal $mol^{-1}$)

| Complex **I**@CB [7] | $\Delta E_{total}$ | $\Delta E_{vdW}$ |
|---|---|---|
| The N–O bond of **I** in the cavity is parallel to the portals (Fig. 5) and corresponds to the maximum complexation energy | −43.3 | −28.6 |
| The N–O bond of **I** in the cavity is parallel to the $C_7$ symmetry axis of the CB [7] molecule | −34.9 | −36.6 |

**Table 4.** Charges on the N and O atoms of the NO group in free **I** ($q_{free}$) and in the complex ($q_{comp}$) for two orientations of **I** in the CB [7] cavity. Spin densities (*sd*) on N and O atoms of the NO group in free **I** ($sdN_{free}$, $sdO_{free}$) and in **I**@CB [7] complexes ($sdN_{comp}$, $sdO_{comp}$)

| | $q_{free}/q_{comp}$ | $qN_{free}/qN_{comp}$ | $qO_{free}/qO_{comp}$ | $sdN/sdN_{comp}$ | $sdO/sdO_{comp}$ |
|---|---|---|---|---|---|
| N–O is parallel to portals | –0.123 | –0.044/–0.038 | –0.274/–0.305 | 0.437/0.466 | $sdO/sdO_{comp}$ |
| N–O is parallel to $C_7$ axis | –0.055 | –0.044/–0.051 | –0.274/–0.263 | 0.437/0.433 | 0.437/0.433 |

ferricyanide $K_3[Fe(CN)_6]^{3-}$. The advantage of these broadening reagents is large negative charges of the anions, whereby they should not bind to CB [7] having a negative surface potential. The values of the exchange broadening in the spectra of free **I** and the complex **I**@CB [7], which are caused by Crox, are given in Table 2. The degree of accessibility of Crox to the NO group of **I** in the complex **I**@CB [7] can be estimated from the ratio $\Delta\omega_{com}^{ex}/\Delta\omega_{free}^{ex}$. It can be seen from Table 2 that this value for probe **I** is rather small.

**Aggregation of I@CB [7] complexes in the presence of chaotropic reagents**. A careful analysis of the ESR spectra of the complex **I**@CB [7] in the presence of Crox reveals additional changes in the line shape, which are not related to the spin-exchange broadening. First, in the absence of Crox, as noted above, the rotational diffusion of the complex **I**@CB [7] is anisotropic, with the fastest rotation occurring about the *Y* axis. However, in the presence of Crox, the shape of the ESR spectrum corresponds to almost isotropic rotation. In addition, the ratio of the intensities of the HFC components $I_{+1}/I_{-1}$ in the presence of 5 and 10 mmol $L^{-1}$ Crox increases from 1.06 to 1.23 and 1.24, respectively, which indicates an increase in the correlation time of rotation. Furthermore, in the presence of 10 mmol $L^{-1}$ Crox, the $a_N$ value increases from 16.01 to 16.2 G, which indicates an increase in the polarity of the environment of the NO group. Finally, the intensity of the ESR signal decreases to unobservable values in times of 15–60 min, depending on the concentrations of CB [7] and Crox, that is, the decay becomes faster with increasing the concentrations of CB [7] and Crox.

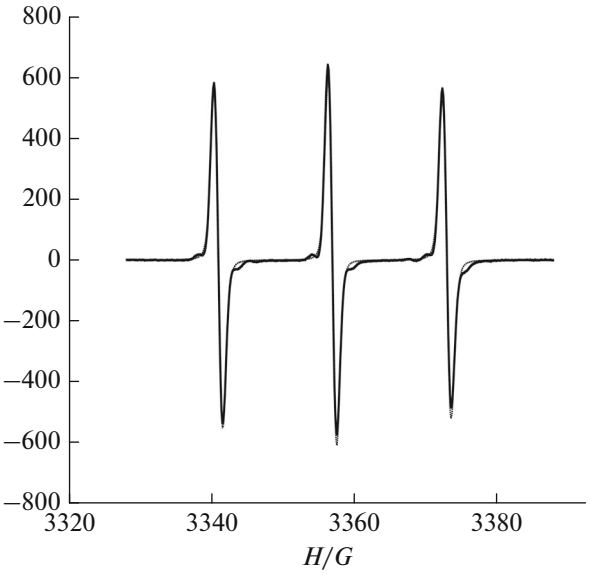


**Fig. 1.** Experimental ESR spectra of the complex **I**@CB [7] in aqueous solution (solid lines) and calculated ESR spectra (dashed lines) corresponding to the best agreement with the experimental spectra in the model of fast diffusional rotation about the *Y* axis in the system of the principal axes of the *A*, *g* tensors. The rotational diffusion coefficients of **I** about the *Y* axis and the axes perpendicular to it are $3.5 \times 10^{10}$ and $6.3 \times 10^{8}$ $s^{-1}$, respectively.

The most probable explanation for these spectral changes is the interaction of **I**@CB [7] molecules with free CB [7] in the presence of Crox, leading to the formation and precipitation of aggregates formed. It is important that this process does not occur with HG complexes of some other radicals with CB [7] (the respective results will be considered in our next work). The formation of aggregates apparently requires some stereoregularity, that is, guest-undisturbed CB [7] portals and the lack of electrostatic repulsion. These conditions are realized for the complexes **I**@CB [7] in which **I** is completely included in the CB [7] cavity, but not for the radicals that are charged or partially exposed to the aqueous phase. An increase in the aggregation degree leads to precipitation of large aggregates and decay of the ESR signal. The aggregates of smaller size contribute to the ESR signal in the solution; they are responsible for changing the anisotropy and increasing the correlation time of rotation. Broadening of the ESR lines due to rotational relaxation means that the actual rate of spin exchange with Crox anions is somewhat smaller than the value given in Table 2.

In addition to Crox, we used potassium ferricyanide (PF) as a broadening reagent. In this case, the ESR signal disappeared almost immediately after the addition of 5 mmol $L^{-1}$ PF to the solution of **I**@CB [7] in excess CB [7]. We assume that the reason for the aggregation induced by Crox or PF is the chaotropic properties of these compounds: aggregation of **I**@CB [7] and free CB [7] under the action of Crox and PF occurs due to destruction of the hydrogen bond network that impeded this aggregation in their absence. Another possible cause of the effect of Crox and PF on the aggregation is an increase in the ionic strength or binding $K^+$ cations to the CB [7] surface, which leads

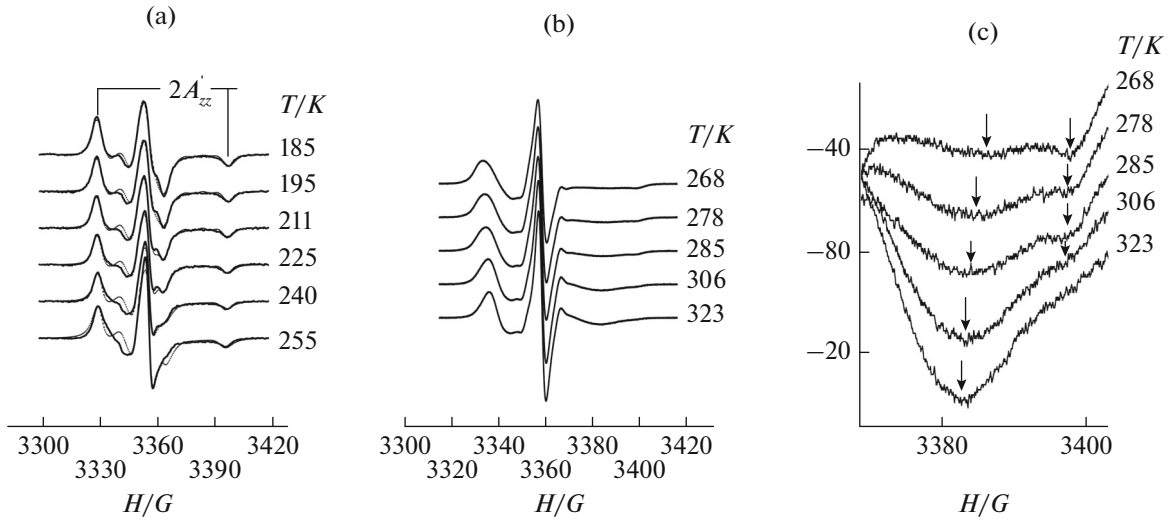


**Fig. 2.** Temperature dependences of the ESR spectra of the complex **I**@CB [7] in the solid CB [7] matrix. (a) Experimental (solid lines) and best calculated (dashed lines) ESR spectra in the low-temperature region. The CB [7]/**I** molar ratio is 60. (b), (c) High-temperature and high-temperature upfield regions, respectively.

to a decrease in the electrostatic repulsion of CB [7] molecules and increasing the aggregation.

We tested this explanation by precipitation of the assumed aggregates on a centrifuge. The sediment is really formed, and the ESR spectrum of its suspension in water corresponds to the region of slow rotation of **I**; the distance between the terminal extremums of the spectrum, equal to the motion-averaged parameter $2A'_{zz}$ at 293 K, is about 66 G, which practically coincides with the value for the complex **I**@CB [7] in the solid CB [7] matrix (Fig. 2a).

### *Properties of the Complex **I**@CB [7] in the Solid CB [7] Matrix*

**Polarity of the environment of the NO group for the complex I@CB [7] in the solid CB [7] matrix.** As the spectral parameter sensitive to the polarity of the environment, we used the distance between the terminal extremums of the ESR spectrum at 77 K, which with a sufficiently high accuracy is twice the *zz* component of the HFC tensor ($A_{zz}$). The dimensionless polarity parameter in the solid CB [7] matrix was determined similarly to the polarity parameter in the aqueous solution of the complex:

$$p_{\text{solid}} = (A_{zz}^{CB} - A_{zz}^{T})/(A_{zz}^{W} - A_{zz}^{T}), \qquad (3)$$

where the upper indices *CB*, *T*, and *W* refer to the complex, toluene, and water. The values of these parameters are given in Table 1.

It is clear from the comparison of the parameters $p_{\text{solid}}$ and $p_{\text{solut}}$ that the local environment of **I** in the complex **I**@CB [7] located in the solid CB [7] matrix is much more hydrophobic than in the complex located in the water environment. These differences are obviously due to the lack of water in the solid CB [7] matrix. The anhydrous environment can also cause changes in the localization of probe **I** in the cavity. To reveal these changes, calculations by the DFT method in the absence and in the presence of water in the environment of the complex are necessary.

**Rotational mobility of I in the complex I@CB [7] in the CB [7] matrix.** It can be seen from Fig. 2 that the shape of the ESR line of radical **I** in the temperature range of 142–340 K corresponds to the region of slow rotation; the most pronounced change in the spectrum with increasing temperature is a decrease in the parameter $2A'_{zz}$. We performed simulation of the spectra in terms of the model of Brownian rotational diffusion. The values of the $A_{zz}$ and $g_{zz}$ components of the HFC and *g*-factor tensors were measured at 77 K; the values of other components were taken from the literature data [9]. Figure 2 also shows the best calculated spectra for the complex **I**@CB [7].

It can be seen from Fig. 2a that at low temperatures the simulation is satisfactory, but with increasing temperature, the agreement with the experiment deteriorates. In particular, at $T > 260$ K, the upfield portion of the spectrum is greatly broadened (Fig. 2b). In addition, a careful study reveals two minimums in the upfield portion of the spectrum, which indicate the existence of two states with different rotational mobility. With increasing temperature, the strongly immobilized component, which corresponds to a larger $A'_{zz}$ value, is transformed into a weakly immobilized component characterized by a much larger broadening of the minimum $m = -1$ (Fig. 2c). In the temperature range of 270–315 K, both components are observed.

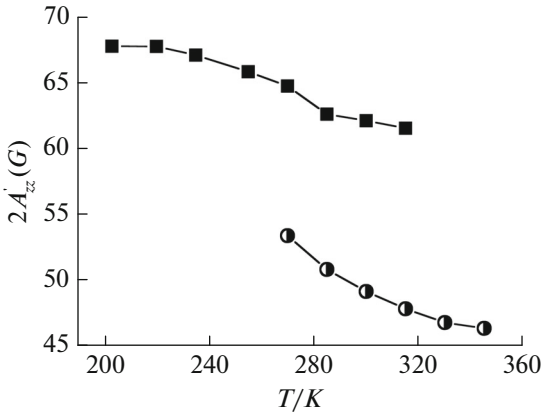


**Fig. 3.** Temperature dependences of the parameter $2A'_{zz}$ (G) of probe **I** in the complex **I**@CB [7] in the solid CB [7] matrix.

Figure 3 shows the changes in the parameters $2A'_{zz}$ with temperature.

The simultaneous existence of two states with different rotational mobility of the guest and transition from a strongly immobilized to weakly immobilized state with growing temperature indicate structural rearrangement in the complex. Elucidation of the nature of this rearrangement requires further investigation.

Here we consider the properties of the weakly immobilized state in more detail for temperatures at which the contribution of the strongly immobilized state is negligible. The ESR spectra were simulated for various types of anisotropic rotation: isotropic, *X*-, *Y*-, and *Z*-axial rotations. The best fitting was obtained for the model of fast axial rotation about the *Y* axis. It is important to note that a significant improvement of the fitting was achieved for the model of jump-like large-angle rotation. It is this feature that is responsible for the large broadening of the spectral minimum in a high field with increasing temperature (Fig. 4a).

The conclusion about the *Y*-axial rotation agrees with the calculations of the structure of the complex **I**@CB [7] by the DFT method. Note that the comparison with calculations by the DFT method for "gas phase", that is, in a nonpolar medium is justified in this case, because the complex **I**@CB [7] is embedded in the hydrophobic CB [7] matrix. The hydrophobic environment created by this matrix is deduced, first, from the low solubility of CB [7] in water. Second, the nitroxyl radical was introduced into the solid CB [7] matrix, which dissociated from the CB [7] cavity at high temperature. The ESR spectrum of this radical corresponded to rapid rotation and hydrophobic environment.

Simulation of the ESR spectra of **I**@CB [7] in the CB [7] matrix for different temperatures (Fig. 4a) permitted determining the rotational diffusion coefficients for rotation about the *Y* axis ($R_{\|}$). It can be seen from Fig. 4b that the temperature dependence of $R_{\|}$ is rather weak and does not obey the Arrhenius equation.

## RESULTS OF CALCULATIONS

In the presence of hydrophobic environment in the CB [7] cavity, one of the forces holding **I** inside the cavity is the van der Waals interaction. This means that for correct calculation of the structure of the complex, it is necessary to use the DFT method with allowance for the dispersion (van der Waals) interaction. In addi-

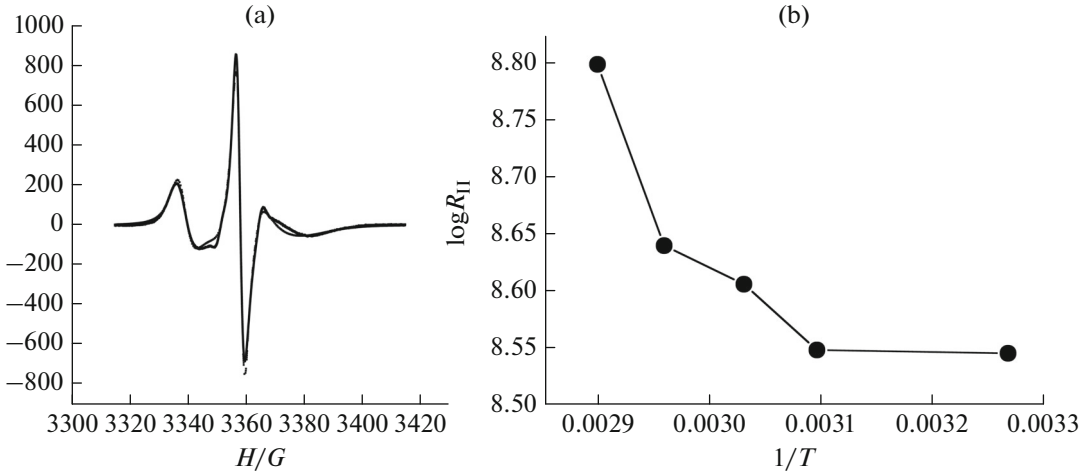


**Fig. 4.** (a) Simulation of the ESR spectrum of the complex **I**@CB [7] in the solid CB [7] matrix in the model of jump-like rotation about the *Y* axis at large angles. The experimental spectrum (solid line) and the calculated spectrum corresponding to the best agreement with the experimental spectrum (dashed line) at a temperature of 338 K. (b) Temperature dependence of the rotational diffusion coefficient for uniaxial rotation about the *Y* axis in the coordinate system of the magnetic tensors of probe **I** in the complex **I**@CB [7].

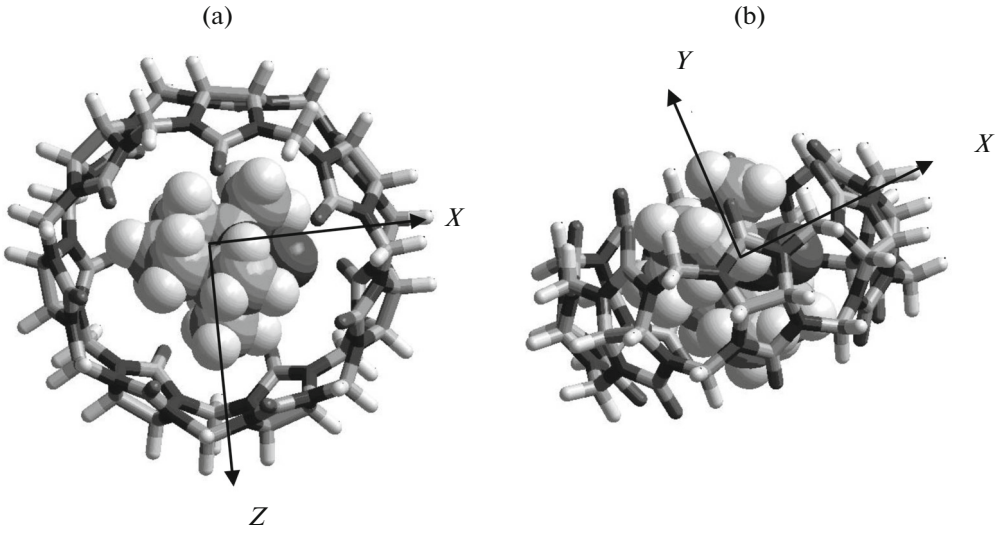


**Fig. 5.** Structure of the complex **I**@CB [7] corresponding to the minimum energy (calculated by the DFT-D method): (a) top view and (b) side view. The NO group of **I** is located in the middle plane parallel to the portals. Colors of guest **I** atoms are dark gray (O and N atoms), gray (C atoms), and light gray (H atoms).

tion, the cavitand CB [7] has seven carbonyl groups in the upper and lower portals, which favors the formation of clouds of negative potential in the portal areas. Therefore, an additional driving force of complexation can be the transfer of electron density from the cavitand to the probe molecule. It should be noted, however, that the complexation energies obtained in this way cannot be directly related to the constant of binding the spin probe to CB [7], since these values do not allow for the entropy term in the free energy of binding. At the same time, they make it possible to characterize the difference in the energies of the complex **I**@CB [7] for different orientations of **I** inside the cavity.

Table 3 presents the energies of the complexation. Figure 5 shows that the most favorable structure of **I**@CB [7], in which the $Y$ axis of the probe is roughly parallel to the $C_7$ symmetry axis of the CB [7] molecule. It is evident from Table 3 that the van der Waals contribution to the total complexation energy for this structure of the complex is more than 2/3 of $\Delta E_{total}$. This means that the calculation of $\Delta E_{total}$ without allowing for $E_{vdW}$ may lead to an underestimated value of $\Delta E_{total}$. For the energetically less favorable structure of **I**@CB [7], in which the N–O bond is parallel to the $C_7$ axis, the value of $\Delta E_{total}$ is less than $\Delta E_{vdW}$, that is, the electronic contribution to the complexation energy is positive. The reason for this fact is that in the latter structure the vectors of the dipole moments of the N–O bond and the C=O groups are roughly parallel, which is energetically unfavorable.

It is evident from the comparison of the charge transfer values presented in Table 4 that the formation of the energetically most favorable structure of **I**@CB [7], in which the polar NO bond is far from the negatively charged CB [7] portals, leads to the transfer of 0.123 of the electron charge to molecule **I**, providing about one third of the total complexation energy. At the same time, for the structure with the orientation of N–O parallel to the $C_7$ axis, the transfer is only 0.055 of the electron charge, which leads to a smaller value of $\Delta E_{total}$ and, in fact, to holding the probe inside the cavity only due to the van der Waals interaction.

The CB [7] molecule consists of seven identical bituril moieties. This means that the structure of **I**@CB [7] (Fig. 5) is sevenfold degenerate, and the energetic profile upon rotation of **I** inside the cavity about the $Y$ and $C_7$ axes in the range of the angles of $0–2\pi$ is described by a periodic potential with seven minimums and maximums. The calculations have shown that the height of the barrier of a rotational hop from one minimum to adjacent is $\approx$1.3 kcal mol$^{-1}$. The small value of the barrier agrees well with the high rotational mobility of the probe detected by us and its weak temperature dependence within the cavity.

Along with the change in the formation energy of the complexes at different orientations of **I** in the CB [7] cavity, we observed changes in the spin density on N and O atoms of the NO group with changing orientation of **I**, which are directly related to a change in the polarity of the environment. Figure 6 shows these changes for the rotation of **I** about the $Z$ axis in the system of principal axes of the $A$, $g$ tensors, where the $Z$ axis coincides with the direction of the $p$ orbits of the NO group of **I**.

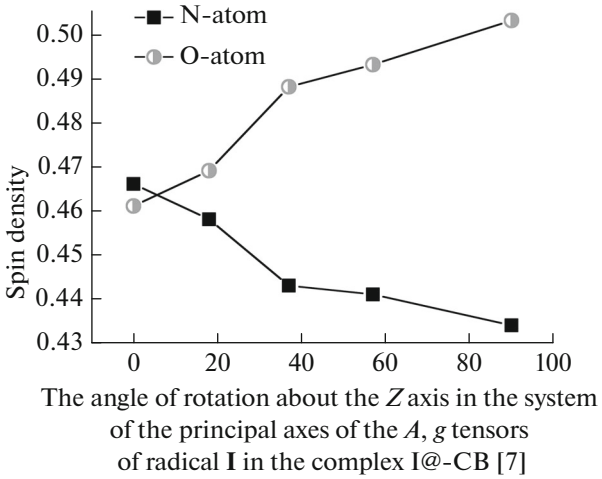


**Fig. 6.** Dependences of the spin densities on the nitrogen and oxygen atoms of the NO group of radical **I** on the angle of rotation about the *Z* axis in the system of the principal axes of the *A*, *g* tensors of **I** in the CB [7] cavity.

## CONCLUSIONS

In summary, the application of the ESR method in combination with quantum-chemical calculations by the DFT method of the host–gest complex of the spin probe TEMPO with cucurbituryl CB [7] in aqueous solution and solid CB [7] matrix permitted determining important dynamic and structural features of this complex.

The kinetic accessibility of the NO group of **I** for water-soluble reagents has been determined. By simulation of the ESR spectra of the complex, its coefficients of anisotropic rotational diffusion have been determined. A large difference in the speed of rotation of the probe about the symmetry axis of the diffusion tensor and that for rotation about the axes perpendicular to it may be explained by the existence of rapid rotation of the probe in the cavity of CB [7]. Aggregation of the complexes in an aqueous solution is found in the presence of multiply charged paramagnetic anions, which apparently is due to chaotropic properties of these anions, that is, destruction of the structure of water, as well as the influence of ionic strength, which causes shielding of the negative potential on the surface of cucurbituril.

It has been shown that the polarity of the environment of the probe in the complex **I**@CB [7] included in the solid CB [7] matrix is much smaller than for the complex in aqueous solution.

Of greatest interest is the high rotational mobility of the guest molecule inside the cavity in the CB [7] plane parallel to the portals, about the *Y* axis in the system of the principal axes of magnetic tensors. (Note that in the time of performing this work, similar results were published on the internal rotation of other guest molecules in the cavity of cucurbituril [13]).

By simulation of the ESR spectra, it has been established that the character of rotation of **I** in the cavity is uncorrelated diffusion jumps at large angles, which agrees with the low value of the rotation barrier ($\approx$1.3 kcal mol$^{-1}$) determined by the DFT method. The nonexponential temperature dependence of the diffusion coefficient (Fig. 4) apparently reflects the change in the rotation barrier for **I** with temperature due to a change in the geometry of the CB [7] molecule itself. Of particular interest is the fact that high rotational mobility takes place despite the rather high binding constant of **I** with CB [7] ($2.5 \times 10^4$ L mol$^{-1}$) and the low accessibility of the guest for water-soluble agents. This property, along with the sensory advantages of cucurbiturils, which are determined by the low polarity of the cavity, makes cucurbiturils promising containers for carrying out chemical, in particular, photochemical processes in nanovolumes.

## ACKNOWLEDGMENTS

This work was supported by the Russian Science Foundation, grant no. 15-13-00163.

## REFERENCES

1. Lagona, J., Mukhopadhayay, P., Chakabarty, S., and Isaacs, L., *Angew. Chem.*, 2005, vol. 117, p. 4922.
2. Isaacs, L., *Chem. Commun.*, 2009, p. 619.
3. Dsouza, R.N., Pischel, U., and Nau, W.M., *Chem. Rev.*, 2011, vol. 111, p. 7941.
4. Wagner, B.D., Stojanovic, N., Day, A.I., and Blanch, R.J., *J. Phys. Chem. B*, 2003, vol. 107, p. 10741.
5. Ivanov, D.A., Petrov, N.Kh., Nikitina, E.A., Basilevski, M.V., Vedernikov, A.L., Gromov, S.P., and Alfimov, M.V., *J. Phys. Chem. A*, 2011, vol. 115, p. 4505.
6. Ong, W. and Kaifer, A.F., *J. Org. Chem.*, 2004, vol. 69, p. 1395.
7. Jeon, Y.J., Kim, H., Jon, S., Selvapalan, N., Oh, D.H., Seo, I., Park, C.S., Jung, S.R., Koh, D.S., and Kim, K., *J. Am. Chem. Soc.*, 2004, vol. 126, p. 15944.
8. Lee, J.W., Kim, S.Y., Kim, H.J., and Kim, K., *Angew. Chem., Int. Ed. Engl.*, 2005, vol. 44, p. 87.
9. Mezzina, E., Cruciani, F., and Pedulli, G.F., Lucarini, M., *Chem.-Eur. J.*, 2007, vol. 13, p. 7223.
10. Jayarai, N., Porel, M., Ottaviani, M.F., Maddipatla, M.V.S.N., Modelli, A., Da Silva, J.P., Bohogala, B.R., Captain, B., Jockusch, S., Turro, N.J., and Ramamurthy, V., *Langmuir*, 2009, vol. 25, no. 24, p. 13820.
11. Spulber, M., Schlick, S., and Villamena, F.A., *J. Phys. Chem. A*, 2012, vol. 116, p. 8475.
12. Bardelang, D., Banaszak, K., Karoui, H., Rockenbauer, A., Waite, M., Udachin, K., Ripmeester, J., Ratcliffe, C., Quari, O., and Tordo, P., *J. Am. Chem. Soc.*, 2009, vol. 131, p. 5402.
13. Casano, G., Poulhis, F., Tran, T.K., Ayhan, M.M., Karoui, H., Siri, D., Gaudel-Siri, A., Rockenbauer, A., Jeschke, G., Bardelang, D., Tordo, P., and Ouari, O., *Nanoscale*, 2015, vol. 7, no. 28, p. 12143.

14. Rozantsev, E.G., *Svobodnye iminoksil'nye radikaly* (Free Iminoxyl Radicals), Moscow: Khimiya, 1970.

15. Fajer, P. and Marsh, D., *J. Magn. Reson.*, 1982, vol. 49, p. 212.

16. Schneider, D.J. and Freed, J.H., *Biological Magnetic Resonance*, vol. 8: *Spin Labeling: Theory and Applications*, Berliner, L.J. and Reuben, J., Eds., New York: Springer, 1989, ch. 1, p. 1.

17. Budil, D., Lee, S., Saxena, S., and Freed, J.H., *J. Magn. Reson., Ser. A*, 1996, vol. 120, p. 155.

18. Neese, F., *Wiley Interdiscip. Rev.: Comput. Mol. Sci.*, 2012, vol. 2, p. 73.

19. Grimme, S., *J. Comput. Chem.,* 2004, vol. 25, p. 1463.

20. Grimme, S., Ehrlich, S., and Goerigk, L., *J. Comput. Chem.*, 2011, vol. 32, p. 1456.

21. Grimme, S., Antony, J., Ehrlich, S., and Krieg, H., *J. Chem. Phys.*, 2010, vol. 132, p. 154104.

22. Griffith, O. and Jost, P., *Spin Labeling: Theory and Applications*, Berliner, L.J., Ed., New York: Academic, 1976, ch. 12, p. 453.

23. Molin, Yu.N., Salikhov, K.M., and Zamaraev, K.I., *Spin Exchange: Principles and Applications in Chemistry and Biology*, New York: Springer, 1980.

24. Yager, T.D., Eaton, G.R., and Eaton, S.S., *J. Chem. Soc., Chem. Commun.*, 1978, p. 944.

*Translated by A. Tatikolov*